ResearchGate

See discussions, stats, and author profiles for this publication at: https://www.researchgate.net/publication/269730095

Borehole thermal energy storage system for heating applications: Thermodynamic performance assessment

Article *in* Energy Conversion and Management · January 2015

DOI: 10.1016/j.enconman.2014.10.043

CITATIONS
42

READS
1,065

2 authors:

Önder Kizilkan
Isparta University of Applied Sciences
52 PUBLICATIONS **878** CITATIONS

SEE PROFILE

Ibrahim Dincer
Ontario Tech University
1,702 PUBLICATIONS **60,531** CITATIONS

SEE PROFILE

Some of the authors of this publication are also working on these related projects:

Project The Sono-Hydro-Gen process (Ultrasound induced hydrogen production) View project

Project Photocatalytic reactor for Cu-Cl cycle View project

All content following this page was uploaded by Önder Kizilkan on 26 September 2018.

The user has requested enhancement of the downloaded file.

Energy Conversion and Management 90 (2015) 53–61

Contents lists available at ScienceDirect

Energy Conversion and Management

journal homepage: www.elsevier.com/locate/enconman

Borehole thermal energy storage system for heating applications: Thermodynamic performance assessment

Onder Kizilkan [a,*], Ibrahim Dincer [b,1]

[a] Süleyman Demirel University, Faculty of Technology, Department of Energy Systems Engineering, 32200 Isparta, Turkey
[b] Faculty of Engineering and Applied Science, University of Ontario Institute of Technology, 2000 Simcoe Street North, Oshawa, Ontario L1H 7K4, Canada

ARTICLE INFO

Article history:
Received 6 March 2014
Accepted 19 October 2014

Keywords:
Borehole thermal energy storage
Energy
Exergy
Efficiency
Heat pump

ABSTRACT

A comprehensive thermodynamic assessment of a borehole thermal energy storage system (BTES), which helps in meeting the heating and cooling demands of campus buildings of University of Ontario Institute of Technology (UOIT), is presented for the heating case. The BTES located on UOIT campus in Oshawa, Canada is recognized as the world's second largest BTES system. Energy and exergy analyses of the heating system are performed through the balance equations, and exergy destruction rates are determined for each system component and the overall BTES. In addition, a comparative system performance assessment is carried out. Based on the conducted research for the studied system, COP_{HP} is calculated to be 2.65 for heating applications. Energy and exergy efficiencies of the boilers are determined to be 83.2% and 35.83%, respectively. The results of the exergy analysis show that the boilers are the major contributor to exergy destruction, followed by condenser and evaporator. The effects of condenser and evaporator temperatures of the heat pump systems on energy and exergy efficiencies are also investigated. The overall exergy efficiency of the whole system is calculated to be 41.35%.

© 2014 Elsevier Ltd. All rights reserved.

1. Introduction

Humankind has been facing great energetic and environmental challenges which urge us to develop potential solutions for every sector of economic activities. As known, one-third of the world's total primary energy is consumed by residential and commercial buildings [1]. Heating and cooling applications represent a major contributor to energy consumption in buildings. For such applications, energy storage systems can contribute substantially to meeting society's demands for more efficient energy usage. Besides, energy storage ensures environmentally-benign energy utilization. The use of energy storage systems includes significant advantages, such as reduced energy costs, reduced energy consumption, better indoor air quality, increased flexibility of operation and reduced pollutant emissions [2] and [3]. It is expected that energy consumption will continue increasing due to the drastic increase in population, industrialization of developing countries, increased use of technologies, etc. The focus has recently been placed on renewables and earth energy options [4].

The use of ground source heat pusmps (GSHPs) in residential and commercial buildings and facilities is considered a remarkable application, since the ground temperature becomes almost constant during the years, after the first upper 5–10 m. The ground is essentially boundless and always existent and as a heat exchange medium it is thermally more consistent than air. This results in a more efficient use of energy for heating applications, and it has been employed as the heat resource in heating, ventilation and air conditioning (HVAC) systems and preparing domestic hot water for both residential and commercial facilities [5] and [6]. GSHP systems are well known systems and have been widely utilized in various countries, including Europe and North America, as one of the important sustainable technologies. Also these systems have become very attractive in some Asian and some other developing countries during the 1990s, since it is substantially treated as advantageous for better energy economy and reduced environmental impacts [7].

In the GSHP, heat absorption is done by circulating the working fluid in borehole heat exchanger (BHE). The working fluid can be water/anti-freeze mixture, or brine that usually circulates in the high density polyethylene pipes installed vertically in boreholes or horizontally in grooves [8]. In numerous applications, it is widespread to fill the gap between borehole wall and pipes with grouting material, while groundwater is frequently used for this aim in some Scandinavian countries. The benefit of using water

* Corresponding author. Working at UOIT as Visiting Associate Professor during the study. Tel.: +90 246 2111409; fax: +90 246 2371283.

E-mail addresses: onderkizilkan@sdu.edu.tr (O. Kizilkan), Ibrahim.Dincer@uoit.ca (I. Dincer).

1 Department of Mechanical Engineering, KFUPM, Dhahran 31261, Saudi Arabia.

http://dx.doi.org/10.1016/j.enconman.2014.10.043
0196-8904/© 2014 Elsevier Ltd. All rights reserved.

Nomenclature

ex	specific exergy (kJ/kg)
$\dot{E}x$	exergy (kW)
$\dot{F}$	fuel energy rate (kW)
h	specific enthalpy (kJ/kg)
$\bar{h}$	specific enthalpy (kJ/kmol)
$\bar{h}^{\circ}$	specific enthalpy at reference state (kJ/kmol)
$\bar{h}_f^{\circ}$	specific enthalpy of formation (kJ/kmol)
HHV	higher heating value (kJ/kg)
LHV	lower heating value (kJ/kg)
$\dot{m}$	mass flow rate (kg/s)
M	molar mass (kg/kmol)
N	number of moles
$\dot{Q}$	heat (kW)
$\dot{P}$	product (kW)
s	specific entropy (kJ/kg K)
$\bar{s}$	specific entropy (kJ/kmol K)
$\bar{s}^{\circ}$	specific entropy at reference state (kJ/kmol)
$\dot{S}$	entropy (kW/K)
T	temperature (°C)
$\dot{W}_C$	compressor power (kW)
$\dot{W}_p$	circulating pump power (kW)
η	efficiency
Subscripts	
0	reference state
B	Boiler
BHE	borehole heat exchanger
BW	BHE side glycol-water solution
ch	chemical
C	condenser
d	destruction
$elec$	electric
E	evaporator
EV	expansion valve
FC	fan-coil system
GEN	generation
HP	heat pump
HW	heating water
$mech$	mechanic
P	product
R	reactant
sys	system

is cheaper mountings and if needed more easy attainment to the collector. On the other hand, grouting is used in many counties in order to strengthen the borehole wall [9].

Recently, various analytical and numerical studies have been conducted by some researchers about BTES systems, mostly concerning with modelling of pipe configurations, investigation of heat transfer characteristics, thermal response tests of different boreholes types, performance tests of ground, etc. A number of them have dealt with thermodynamic analysis of BTES systems for residential and commercial applications. Ozgener et al. [10] carried out energetic and exergetic analysis of the Salihli geothermal district heating system with the actual thermal data. They analyzed the system performance through energy and exergy aspects for determining improvement potentials of the system. The major exergy destruction rates were found in the pumps and heat exchangers. The systems energy efficiency was found to be 55.5% while the exergy efficiency was 59.4%. Esen et al. [6] conducted energy and exergy analysis of a GCHP system using two different horizontal ground heat exchangers (GHE). They analyzed experimentally the effects of the buried depth of the ground coupled heat exchanger on the efficiencies. They found that the energy efficiencies of the system were 2.5 for the first GHE and 2.8 for the second, while the exergetic efficiencies of the system were found to be 53.1% and 56.3%, respectively. Sakulpipatsin et al. [11] presented a method for exergy analysis HVAC systems situated in the Netherlands. They exemplified an office building which was equipped with heating and cooling systems. In their results, the overall exergy efficiencies were found to be 17.15% for heating and 6.81% for cooling. They also noted that there was a big potential to be improved. Zhai and Yang [12] investigated a ground source heat pump system which was constructed in Shanghai. The system consists of two heat pumps with the rated cooling capacity of 500 kW for each and 280 boreholes with 80 m in depth. They reported that operating cost of the GSHP system was lowered by 55.8% when compared with a traditional air source heat pump system. Additionally they analyzed the implementations of GSHP systems for different climatic zones of China. Urchueguía et al. [13] investigated the ground source heat pump systems in terms of technical and economic feasibility for mixed climate applications. For this aim, they implemented an experimental heat pump system with ground source heat exchanger. The air conditioned area of the experimental system was 250 m^2 and heating and cooling loads were 15 kW and 17 kW, respectively. The ground heat exchangers (2 × 3) were 50 m in depth. They found that, ground coupled heat pump system had an energy savings of 43% for heating and 37% for cooling, respectively. Sharqawy et al. [14] investigated a vertical U-shaped GHE with 80 m depth and 20 cm borehole diameter which was installed at KFUPM, Dhahran, Saudi Arabia. They constructed a mobile thermal response test apparatus to the system in order to measure the performance of the GHE. They found the GHE's energy efficiency to be 46.6% and the second law efficiency to be 51.1%. Wu et al., [15] simulated ground source absorption heat pumps coupled with borehole for three different cities. They carried out dynamic simulations obtaining soil and water temperatures of the borehole for long-term operation. They found high COP and heating capacity of their proposed systems.

In present study, thermodynamic analysis of the BTES system located in UOIT in Ontario, Canada, is conducted for thermodynamic performance assessment for winter season. In this regard, energy and exergy flows of the system are determined through thermodynamic balance equations to layout the buildings' heat demand pattern. Parametric studies are also performed to determine the effects of various system parameters and operating conditions on energy and exergy efficiencies. Actual data accessed from the operating system in university campus is used for the calculations.

2. System description

The BTES system studied and assessed here is installed on the campus of University of Ontario Institute of Technology in Oshawa, Canada. A schematic representation of this system for heating season is shown in Fig. 1 [16]. The buildings were designed to be cooled and heated with GSHP system. During summer, the fluid circulating through tubing extended into the wells, collects heat from the buildings and carries it to the ground. In winter, the system reverses to take heat from the ground and transmits it into the buildings. For a long time operation the heat load is balanced using cooling towers in summer season. As mentioned earlier, GSHP system equipped with the BTES, in order to reduce energy consumptions, environmental emissions, and financial costs. Aside

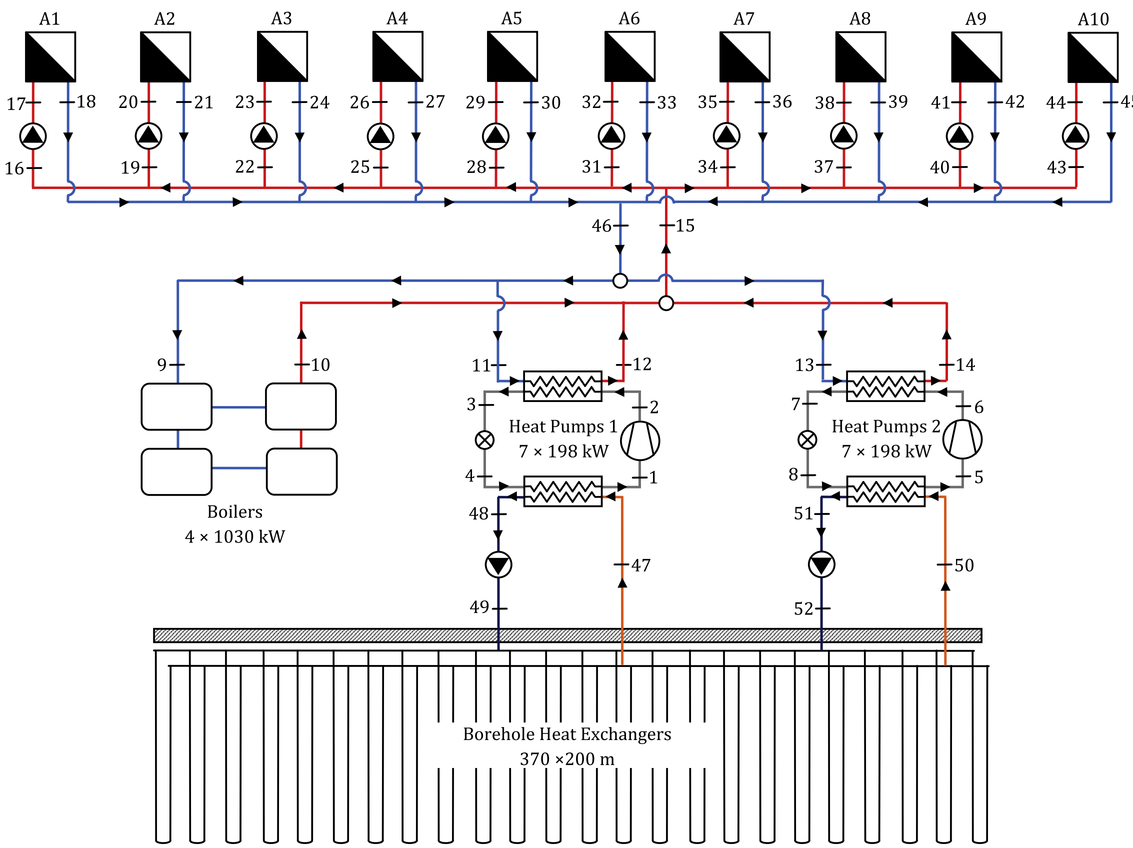

Fig. 1. Schematic illustration of the heating system (modified from Ref. [16]).

from being a major unit of the university's heating and cooling system, the BTES is also used for investigation and education purposes. Additionally, The BTES mentioned here has got the largest and deepest field in Canada, and its geothermal well field is one of the largest in North America [2].

The BTES system coupled with GSHP facility supplies a heating system for the whole campus buildings, utilizing the energy obtained from the ground. Heat pumps are used to pump energy from the BTES system into the buildings. The total heating load of the campus buildings is about 6800 kW. The amount of energy pumped by the heat pumps is about 40% of the overall heating demand of the buildings. The rest of the heating demand is supplied by natural gas boilers as seen in Fig. 1. There are four boilers which are 1030 kW in capacity and have efficiency of 95% [16], [17] and [18]. The refrigerant R407C is used in the GSHP system and the total heat pump capacity is 2770 kW. In order to meet the energy demand of campus buildings, it was determined using the thermal conductivity test results that a field of 370 boreholes, each 200 m in depth, would be required. Instead of the North American application of grouted BHEs, the Swedish application of water-filled BHEs was employed [19]. Further details are available elsewhere [2], [16], [17], [18] and [19].

As seen from Fig. 1, BHEs are embedded under the ground which consist of polyethylene pipes and filled with 15% glycol solution that circulates through the underground pipe network. Inlet and outlet temperatures of the solution are 5.6 °C and 9.3 °C, respectively. The evaporator water (15% glycol solution) goes into the borehole field and heat energy is absorbed from the borehole water by the evaporator and transferred to the refrigerant. By the help of heat pumps, the energy is transferred to secondary fluid for carrying heat energy to the buildings. For the secondary fluid, 30% glycol solution is used and it is circulated between the heating system and the buildings. In Fig. 1, the top subplot represents the ten campus buildings from A1 to A10. The inlet and exit temperatures of the solution to/from the fan-coils in buildings are 52 °C and 41.3 °C respectively. When the heating load is bigger than the heat pumps' capacity, natural gas boilers take place and support the heat pumps by heating the secondary fluid. The analyses conducted here are carried out for 10 buildings while the university campus currently consists of seven buildings, since the whole system was planned and constructed for 10 buildings [16], [17], [18] and [19].

3. Thermodynamic analysis

For determining the performance characteristics of the GSHP system coupled with BTES, energy and exergy balance equations are employed assuming the system to be steady-state, steady-flow process. The assumptions below are made for the thermodynamic performance assessment of the system:

(a) The changes in potential and kinetic energies are neglected.
(b) The heat transfer and pressure drops in the heat pump pipes are neglected.
(c) The power consumption of fans on the fan-coils is neglected.
(d) The combustion in the boilers is complete, and the combustion process takes place in the stoichiometric conditions.
(e) The air and the combustion gases are ideal gases.
(f) The processes taking place in compressors and expansion valves are adiabatic.
(g) The compressors' isentropic efficiencies of the GSHP system are taken to be 85%.
(h) The mechanical efficiencies of the compressors are taken to be 80% while the electrical efficiencies are taken to be 84%.

(i) The mechanical and electrical efficiencies of the circulating pumps are taken to be 85% and 88%, respectively
(j) The excess air for the boilers is 25%.
(k) The reference state temperature and pressure are taken to be 1.5 °C and 101.325 kPa, respectively.

Under the assumptions listed above, mass, energy and exergy balance equations are applied to determine the rate of the energy and exergy flows of GSHP system.

3.1. Energy analysis

The mass balance equation can be expressed in the rate form as;

$$\sum \dot{m}_{in} = \sum \dot{m}_{out} \tag{1}$$

where $\dot{m}$ is the mass flow rate, subscript in and out represents inlet and outlet respectively. The general energy balance that is the first law of thermodynamics can be expressed as;

$$\dot{Q} - \dot{W} = \sum \dot{m}_{out}h_{out} - \sum \dot{m}_{in}h_{in} \tag{2}$$

where $\dot{Q}$ and $\dot{W}$ denote heat and work, respectively. For combustion process in the boilers, the energy balance under steady-flow conditions with $\dot{W} = 0$ is given by [20]:

$$h_P - h_R = \frac{\sum N_P(\bar{h}_f^\circ + \bar{h} - \bar{h}^\circ)_P - \sum N_R(\bar{h}_f^\circ + \bar{h} - \bar{h}^\circ)_R}{M} \tag{3}$$

where $\bar{h}_f^\circ$ is specific enthalpy of formation, $\bar{h}^\circ$ is specific enthalpy for dead state and $\bar{h}$ is specific enthalpy. N stands for number of moles, M stands for atomic mass and subscripts R and P represents reactants and products, respectively.

The rate of heat extracted from the ground by BHEs ($\dot{Q}_{BHE}$) is determined by

$$\dot{Q}_{BHE} = \dot{m}_{BW}C_{p,BW}(T_{BW,out} - T_{BW,in}) \tag{4}$$

where subscript BW stands for borehole water. The rate of heat absorbed by the evaporator is written as

$$\dot{Q}_E = \dot{m}_R(h_{E,out} - h_{E,in}) \tag{5}$$

where $\dot{m}_R$ is the mass flow rate of the refrigerant. The heat rejection rate in the condenser becomes

$$\dot{Q}_C = \dot{m}_R(h_{C,out} - h_{C,in}) \tag{6}$$

The space heating loads of campus buildings are calculated by

$$\dot{Q}_{FC} = \dot{m}_{HW}C_{p,HW}(T_{HW,out} - T_{HW,in}) \tag{7}$$

The rate of work input to compressor is given as

$$\dot{W}_C = \frac{\dot{m}_R\left(h_{\dot{W}_C,out} - \dot{h}_{\dot{W}_C,in}\right)}{\eta_{W_c,mech}\eta_{W_c,elec}} \tag{8}$$

The rate of work input to circulating pumps is written as

$$\dot{W}_p = \frac{\dot{m}_{HW}(h_{HW,out,pump} - h_{HW,in,pump})}{\eta_{p,mech}\eta_{p,elec}} \tag{9}$$

The coefficient of performance (COP) value can be used for evaluation of the energy performance of the heat pump system. COP is defined as the ratio of the condenser capacity to total energy consumptions of the compressor and the pumps:

$$COP_{HP} = \frac{\dot{Q}_C}{\dot{W}_C + \dot{W}_P} \tag{10}$$

Note that natural gas is currently being used in boilers and for thermodynamic calculations, the properties of methane (CH_4) is used. The higher heating value (*HHV*) of methane is taken to be 55530 kJ/kg and lower heating value (*LHV*) is taken to be 50050 kJ/kg [21]. Air is in standard atmospheric conditions, it could be schematized as composed only by oxygen and nitrogen. Combustion process is assumed to be in stoichiometric conditions and with the excess air of 25%, the following chemical reaction is occurred in the combustion chamber for one mole of methane:

$$CH_4 + 2.5(O_2 + 3.76N_2) \rightarrow CO_2 + 2H_2O + 0.5O_2 + 9.4N_2 \tag{11}$$

During the combustion process, the heat transferred to the heating water from boiler is calculated by:

$$\dot{Q}_B = \dot{m}_{CH_4}(h_R - h_P) = \dot{m}_{CH_4}\frac{\sum N_R(\bar{h}_f^\circ + \bar{h} - \bar{h}^\circ)_R - \sum N_P(\bar{h}_f^\circ + \bar{h} - \bar{h}^\circ)_P}{M_{CH_4}} \tag{12}$$

The energy efficiency of the overall boilers can be obtained by using the equation below.

$$\eta_B = \frac{\dot{Q}_B}{HHV} \tag{13}$$

3.2. Exergy analysis

For exergy analysis, the general exergy balance involving chemical reactions can be expressed as

$$\Delta Ex_{sys} = \sum \dot{E}x_{in} - \sum \dot{E}x_{out} - \dot{E}x_{dest} \tag{14}$$

Table 1
Exergy balance equations for system components.

Component	Exergy balance equation	Entropy balance equation	Exergetic efficiency
Compressor	$\dot{E}x_{dest,W_C} = \dot{E}x_{W_C,in} - \dot{E}x_{W_C,out} + \dot{W}_C$	$\dot{E}x_{dest,W_C} = T_0\left(\dot{S}_{W_C,out} - \dot{S}_{W_C,in}\right)$	$\varepsilon_{W_C} = \frac{\dot{E}x_{W_C,out} - \dot{E}x_{W_C,in}}{\dot{W}_C}$
Condenser	$\dot{E}x_{dest,C} = \left(\dot{E}x_{C,in} - \dot{E}x_{C,out}\right) + \left(\dot{E}x_{HW,in} - \dot{E}x_{HW,out}\right)$	$\dot{E}x_{dest,C} = T_0\left[\left(\dot{S}_{C,out} - \dot{S}_{C,in}\right) + \left(\dot{S}_{HW,out} - \dot{S}_{HW,in}\right)\right]$	$\varepsilon_C = \frac{\dot{E}x_{HW,in} - \dot{E}x_{HW,out}}{\dot{E}x_{C,in} - \dot{E}x_{C,out}}$
Expansion valve	$\dot{E}x_{dest,EV} = \dot{E}x_{EV,in} - \dot{E}x_{EV,out}$	$\dot{E}x_{dest,EV} = T_0\left(\dot{S}_{EV,out} - \dot{S}_{EV,in}\right)$	$\varepsilon_{ExV} = \frac{\dot{E}x_{ExpV,out}}{\dot{E}x_{ExpV,in}}$
Evaporator	$\dot{E}x_{dest,E} = \left(\dot{E}x_{E,in} - \dot{E}x_{out}\right) + \left(\dot{E}x_{BW,in} - \dot{E}x_{BW,out}\right)$	$\dot{E}x_{dest,E} = T_0\left[\left(\dot{S}_{E,out} - \dot{S}_{E,in}\right) + \left(\dot{S}_{BW,out} - \dot{S}_{BW,in}\right)\right]$	$\varepsilon_E = \frac{\dot{E}x_{BW,out} - \dot{E}x_{BW,in}}{Ex_{\dot{E},in} - \dot{E}x_{E,out}}$
Fan-coils	$\dot{E}x_{dest,FC} = \left(\dot{E}x_{HW,in} - \dot{E}x_{HW,out}\right) + \dot{E}x_{Q_{FC}}$	$\dot{E}x_{dest,FC} = T_0\left[\left(\dot{S}_{HW,out} - \dot{S}_{HW,in}\right) - \left(\frac{\dot{Q}_{FC}}{T_{FC}}\right)\right]$	$\varepsilon_{FC} = \frac{\dot{E}x_{Q_{FC}}}{\dot{E}x_{HW,out} - \dot{E}x_{HW,in}}$
BHE	$\dot{E}x_{dest,BHE} = \left(\dot{E}x_{BW,in} - \dot{E}x_{BW,out}\right) - \dot{E}x_{Q_{BHE}}$	$\dot{E}x_{dest,BHE} = T_0\left[\left(\dot{S}_{BW,out} - \dot{S}_{BW,in}\right) + \left(\frac{\dot{Q}_{BHE}}{T_{BHE}}\right)\right]$	$\varepsilon_{BHE} = \frac{\dot{E}x_{Q_{BHE}}}{\dot{E}x_{HW,in} - \dot{E}x_{HW,out}}$
Pumps	$\dot{E}x_{dest,W_p} = \dot{E}x_{W_p,in} - \dot{E}x_{W_p,out} + W_p$	$\dot{E}x_{dest,W_p} = T_0\left(\dot{S}_{W_p,out} - \dot{S}_{W_p,in}\right)$	$\varepsilon_{pump} = \frac{\dot{E}x_{W_p,out} - \dot{E}x_{W_p,in}}{W_{pump}}$
Boilers	$\dot{E}x_{dest,B} = \left(\dot{E}x_{HW,in} - \dot{E}x_{HW,out}\right) + \left(\dot{E}x_{ch,P} - \dot{E}x_{ch,R}\right) + \dot{E}x_{Q_P}$	$\dot{E}x_{dest,B} = T_0\left(\dot{S}_{HW,out} - \dot{S}_{HW,in} + \dot{S}_P - \dot{S}_R - \frac{\dot{Q}_P}{T_P}\right)$	$\varepsilon_B = \frac{\left(\dot{E}x_{HW,in} - \dot{E}x_{HW,out}\right)}{\left(\dot{E}x_{ch,P} - \dot{E}x_{ch,R}\right)}$

where $\dot{E}x_{in}$ and $\dot{E}x_{out}$ are the rate of net exergy transferred by heat, work and mass, and $\dot{E}x_{dest}$ is the rate of exergy destruction. ΔEx_{sys} equals zero for steady-state process, so Eq. (14) becomes

$$\dot{E}x_Q - \dot{E}x_W + \dot{E}x_{mass,in} - \dot{E}x_{mass,out} = \dot{E}x_{dest} \tag{15}$$

Here, $\dot{E}x_Q$ is the exergy of heat, $\dot{E}x_W$ is the exergy of work and $\dot{E}x_{mass}$ is the exergy of mass flow:

$$\dot{E}x_Q = \dot{Q}\left(1 - \frac{T_0}{T}\right) \tag{16}$$

$$\dot{E}x_W = \dot{W} \tag{17}$$

$$\dot{E}x_{mass} = \dot{m}\, ex \tag{18}$$

where ex is the specific flow exergy and defined as

$$ex = (h - h_0) - T_0(s - s_0) + ex_{ch} + \frac{u^2}{2g} + (Z - Z_0)g \tag{19}$$

where 0 stands for dead state properties at pressure P_0 and temperature T_0. In most cases kinetic and potential components for exergy equation are usually neglected. With this assumption, the chemical exergy term for a steady-state combustion process can be written as

Table 2
Property data calculated for each state of the BTES system.

Number	Fluid	Phase	Temperature (°C)	Mass flow rate (kg/s)	Enthalpy (kJ/kg)	Entropy (kJ/kg K)	Specific exergy (kJ/kg)	Exergy (kW)
0	Water (15%)[a]	Dead state	1.5	–	27.54	0.1012	–	–
0′	Water (30%)[b]	Dead state	1.5	–	58.6	0.2195	–	–
0‴	R407C	Dead state	1.5	–	273.3	1.181	–	–
1	R407C	Superheated vapor	1	7.234	268.3	1.034	34.65	250.6
2	R407C	Superheated vapor	77.24	7.234	316.8	1.055	77.36	559.6
3	R407C	Subcooled liquid	45	7.234	125.2	0.4576	49.83	360.5
4	R407C	Wet vapor	-4	7.234	125.2	0.4895	41.06	297
5	R407C	Superheated vapor	1	7.234	268.3	1.034	34.65	250.6
6	R407C	Superheated vapor	77.24	7.234	316.8	1.055	77.36	559.6
7	R407C	Subcooled liquid	45	7.234	125.2	0.4576	49.83	360.5
8	R407C	Wet vapor	-4	7.234	125.2	0.4895	41.06	297
9	Water (30%)	Liquid	41.3	101.5	206.7	0.723	9.845	999.4
10	Water (30%)	Liquid	52	101.5	247.3	0.8499	15.57	1581
11	Water (30%)	Liquid	41.3	34.15	206.7	0.723	9.845	336.2
12	Water (30%)	Liquid	52	34.15	247.3	0.8499	15.57	531.8
13	Water (30%)	Liquid	41.3	34.15	206.7	0.723	9.845	336.2
14	Water (30%)	Liquid	52	34.15	247.3	0.8499	15.57	531.8
15	Water (30%)	Liquid	52	169.8	247.3	0.8499	15.57	2644
16	Water (30%)	Liquid	52	22.2	247.3	0.8499	15.57	345.7
17	Water (30%)	Liquid	52.01	22.2	247.4	0.8501	15.58	345.9
18	Water (30%)	Liquid	41.3	22.2	206.7	0.723	9.845	218.6
19	Water (30%)	Liquid	52	24.81	247.3	0.8499	15.57	386.4
20	Water (30%)	Liquid	52.02	24.81	247.4	0.8502	15.59	386.7
21	Water (30%)	Liquid	41.3	24.81	206.7	0.723	9.845	244.3
22	Water (30%)	Liquid	52	24.09	247.3	0.8499	15.57	375.1
23	Water (30%)	Liquid	52.03	24.09	247.4	0.8503	15.59	375.6
24	Water (30%)	Liquid	41.3	24.09	206.7	0.723	9.845	237.1
25	Water (30%)	Liquid	52	22.2	247.3	0.8499	15.57	345.7
26	Water (30%)	Liquid	52.02	22.2	247.4	0.8502	15.59	346
27	Water (30%)	Liquid	41.3	22.2	206.7	0.723	9.845	218.6
28	Water (30%)	Liquid	52	22.2	247.3	0.8499	15.57	345.7
29	Water (30%)	Liquid	52.02	22.2	247.4	0.8502	15.59	346
30	Water (30%)	Liquid	41.3	22.2	206.7	0.723	9.845	218.6
31	Water (30%)	Liquid	52	7.764	247.3	0.8499	15.57	120.9
32	Water (30%)	Liquid	52.03	7.764	247.4	0.8503	15.59	121.1
33	Water (30%)	Liquid	41.3	7.764	206.7	0.723	9.845	76.44
34	Water (30%)	Liquid	52	6.353	247.3	0.8499	15.57	98.94
35	Water (30%)	Liquid	52.02	6.353	247.4	0.8501	15.59	99.01
36	Water (30%)	Liquid	41.3	6.353	206.7	0.723	9.845	62.54
37	Water (30%)	Liquid	52	18.87	247.3	0.8499	15.57	293.9
38	Water (30%)	Liquid	52.01	18.87	247.4	0.8501	15.58	294.1
39	Water (30%)	Liquid	41.3	18.87	206.7	0.723	9.845	185.8
40	Water (30%)	Liquid	52	10.44	247.3	0.8499	15.57	162.6
41	Water (30%)	Liquid	52.02	10.44	247.4	0.8501	15.58	162.7
42	Water (30%)	Liquid	41.3	10.44	206.7	0.723	9.845	102.8
43	Water (30%)	Liquid	52	10.88	247.3	0.8499	15.57	169.4
44	Water (30%)	Liquid	52.02	10.88	247.4	0.8502	15.59	169.6
45	Water (30%)	Liquid	41.3	10.88	206.7	0.723	9.845	107.1
46	Water (30%)	Liquid	41.3	169.8	206.7	0.723	9.845	1672
47	Water (15%)	Liquid	9.3	70.67	58.42	0.212	0.43	30.39
48	Water (15%)	Liquid	5.6	70.67	43.76	0.1598	0.1201	8.491
49	Water (15%)	Liquid	5.601	70.67	43.76	0.1598	0.1202	8.493
50	Water (15%)	Liquid	9.3	70.67	58.42	0.212	0.43	30.39
51	Water (15%)	Liquid	5.6	70.67	43.76	0.1598	0.1201	8.491
52	Water (15%)	Liquid	5.601	70.67	43.76	0.1598	0.1202	8.493

[a] 15% glycol–water solution,
[b] 30% glycol–water solution.

$$ex_{ch} = \frac{\sum N_P\left(\bar{h}_f^\circ + \bar{h} - \bar{h}^\circ - T_0\bar{s}\right)_P - \sum N_R\left(\bar{h}_f^\circ + \bar{h} - \bar{h}^\circ - T_0\bar{s}\right)_R}{M} \quad (20)$$

where $\bar{s}$ is specific entropy in kJ/kmol K.

By rearranging the equations given above, general exergy balance equation becomes:

$$\dot{E}x_{dest} = \sum \dot{Q}\left(1 - \frac{T_0}{T}\right) - \dot{W} + \sum (\dot{m}\,ex)_{in} - \sum (\dot{m}\,ex)_{out} + \sum (\dot{m}\,ex_{ch})_{in} - \sum (\dot{m}\,ex_{ch})_{out} \quad (21)$$

Here, $\dot{E}x_{dest}$ term can be also written in terms of entropy generation:

$$\dot{E}x_{dest} = T_0 S_{GEN} \quad (22)$$

For a chemical process such as combustion, the exergy destruction rate can be written as;

$$\dot{S}_{GEN} = \dot{S}_P - \dot{S}_R + \frac{\dot{Q}_{out}}{T} \quad (23)$$

where

$$\dot{S}_P - \dot{S}_R = \dot{m}\frac{\sum N_P\bar{s}_P - \sum N_R\bar{s}_R}{M} \quad (24)$$

For calculation of entropy of the combustion process, temperature and the partial pressure of the component is used. Entropy equation for a component in a combustion process is given as

$$\bar{s}_i(T, P_i) = \bar{s}_i^\circ(T, P_0) - R_u\frac{y_i P_m}{P_0} \quad (25)$$

where P_i is the partial pressure, y_i is the mole fraction of the component i and P_m is the total pressure of the mixture.

In order to determine the exergy efficiency, the ratio of total exergy output to total exergy input is used:

$$\varepsilon_{sys} = \frac{\dot{E}x_{output}}{\dot{E}x_{input}} \quad (26)$$

The general exergy and entropy balance equations for all components of the system, which is illustrated in Fig. 1, are given in Table 1. The balance equations are obtained by employing the general exergy balance equations given above.

4. Results and discussion

A thermodynamic performance assessment of the heating system of university campus buildings is investigated using energy and exergy analysis. Under the assumptions made and using the actual heating load of the university campus buildings, the calculated properties for BTES system are given in Table 2, according to reference points illustrated in Fig. 1. The calculated results of exergy destruction rates, relative irreversibility and exergy efficiencies of system components and overall system are given in Table 3 for comparison. The heating coefficient of performance of the heat pump unit (COP_{HP}) is calculated from Eq. (10) and is found to be 2.65. The rest of the heating demand of campus buildings are supplied by natural gas boilers as stated above. Overall energy efficiency of the boilers is determined to be 83.2% using Eq. (13). This means that 16.8% of heat is lost through boilers walls and by flue gases.

The results of exergy analysis show that the major exergy destruction rate occurs in boilers. Thus, exergy destruction of the boilers is equal to 1041.4 kW with the efficiency of 35.83%. Exergy destruction is high due to the boilers are not fully adiabatic. The other major exergy destruction occurs in fan-coils, followed by compressors, evaporators and expansion valves. In addition, the exergy efficiency of the overall heating system is calculated to be 41.35%. These results match the actual systems conditions.

According to the system characteristics, the BTES system is designed to be economically beneficial. The results have shown that annual energy savings by 40% for heating and 16% for cooling can be achieved using the BTES system when compared to traditional heat pump systems. The system also yielded other indirect financial benefits, such as; reduced boiler plant costs, reduced use of potable water, reduced use of chemicals for the treatment of water, eliminated costs for roof cooling towers and associated building support [2].

Additionally, a parametric study is also carried out for the heating system in order to understand how the system parameters affect the system performance. For the GSHP system, the variations of COP_{HP} with evaporator and condenser temperatures are given in Figs. 2 and 3. As can be seen from the figures, the value of COP_{HP} increases with an increase of T_E and hence decreases with T_C. In heat pumps, smaller entropy generation leads to larger COP_{HP}. It means, entropy generation decreases with increasing evaporator temperature and vice versa for the condenser temperature.

For determining the trend of the boilers' energy performance, excess air ratio and the product temperature values are varied. With the increase of both excess air ratio and product temperature, the overall efficiency of the boilers tends to decrease (Figs. 4 and 5). It is important to mention that a few studies have only been done on exergy and energy analyses of BTES for heating applications by considering completely different systems and different operating conditions which make it difficult to provide comparison between this system and others.

Note that exergy values are strictly connected to the intensive properties of the dead state. The dead state is a state of a system in which it is at equilibrium with its surroundings. Before applying exergy analyses to engineering systems, the significance of the

Table 3
The results of exergetic assessment of BTES system.

Component	Exergy destruction rate (kW)	Exergy efficiency (%)	Relative irreversibility (%)
Boilers	1041.4	35.83	43.68
Compressors	425.6	59.22	17.85
Condensers	7.016	98.24	0.29
Expansion valves	126.9	82.4	5.32
Evaporators	136.6	47.19	5.73
Fan-coils	582.1	40.15	24.42
BHE	53.2	45.14	2.23
Pumps	11.4	13.23	0.48
Overall	2384.2	41.35	–

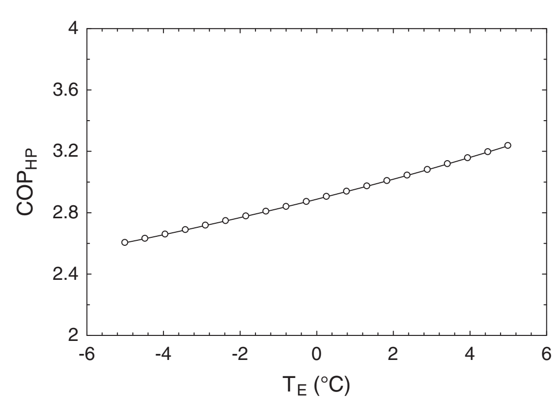

Fig. 2. Variation of COP_{HP} with evaporator temperature.

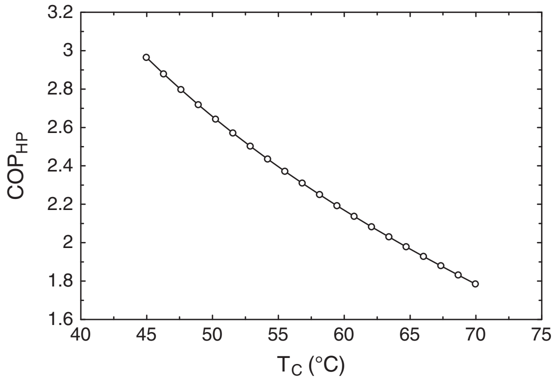

Fig. 3. Variation of *COP_{HP}* with condenser temperature.

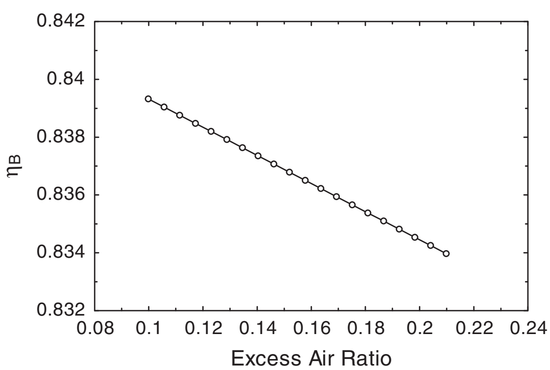

Fig. 4. Variation of boiler efficiency with excess air ratio.

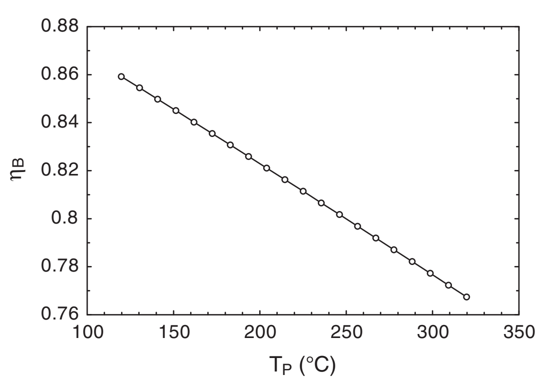

Fig. 5. Variation of boiler efficiency with product temperature.

sensitivities of dead state properties to the results must be assessed [22]. From this point of view, a parametric study is also carried out for determining the trends of exergy analysis results with dead state properties. In Fig. 6, variation of exergy destruction rate and exergy efficiency of the overall system is given with dead state temperature. As can be seen from the figure, the exergy efficiency of the system decreases while exergy destruction increases significantly with the increase of reference temperature. This is because of the increase in the temperature difference between the reference environment and the system. However, this variation does not affect the COP value because it is independent of any change in the reference environment conditions.

Fig. 7 illustrates the variation of exergy destruction results of the heat pump system with the inlet glycol–water temperature.

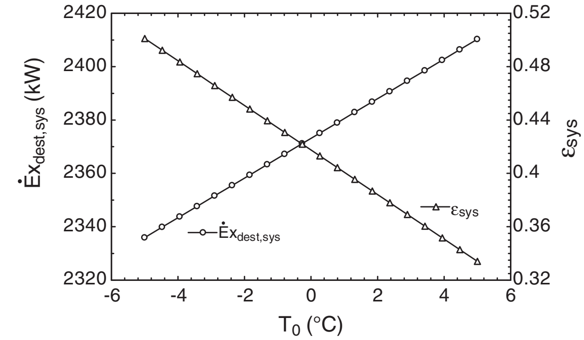

Fig. 6. Variation of exergy destruction and exergetic efficiency with reference temperature.

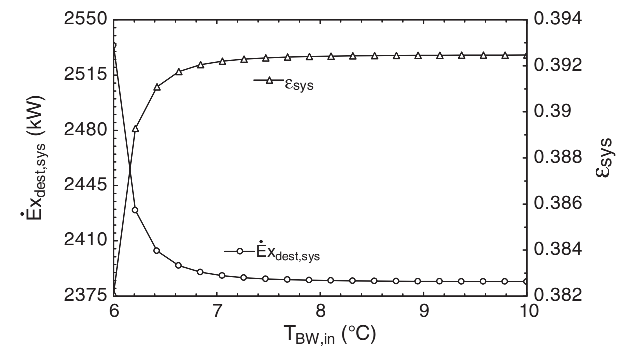

Fig. 7. Variation of exergy destruction and exergetic efficiency with entering glycol–water temperature.

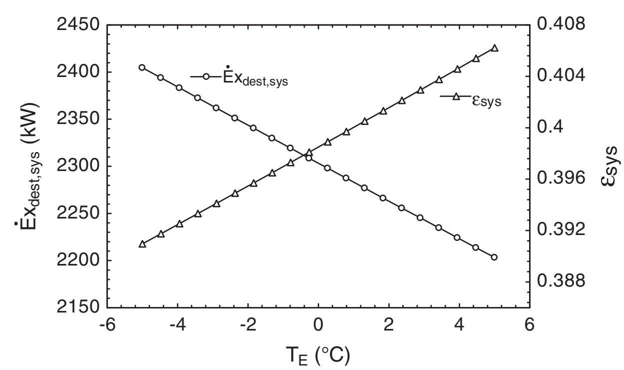

Fig. 8. Variation of exergy destruction and exergetic efficiency with evaporator temperature.

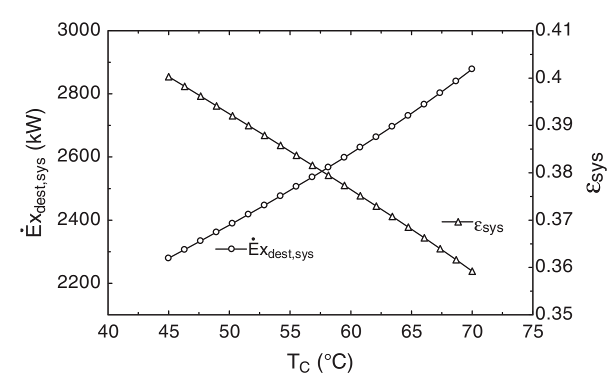

Fig. 9. Variation of exergy destruction and exergetic efficiency with condenser temperature.

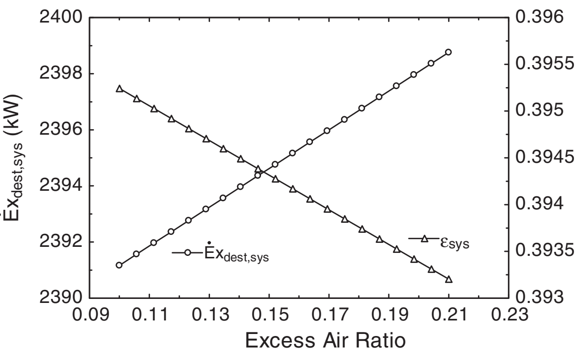

Fig. 10. Variation of exergy destruction and exergetic efficiency with excess air ratio.

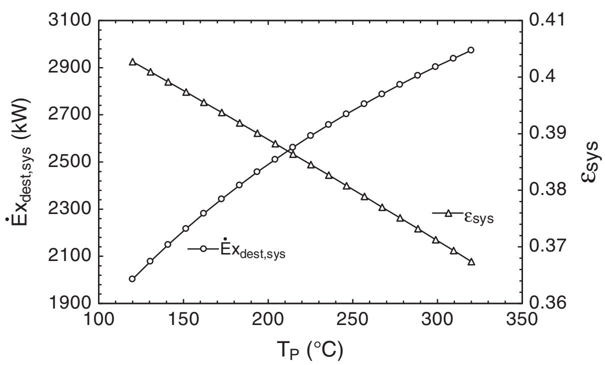

Fig. 11. Variation of exergy destruction and exergetic efficiency with condenser temperature.

The inlet glycol–water temperature to the heat pump system (i.e. evaporator) will be lower than the ambient temperature for winter conditions. With the increase glycol–water temperature entering to the heat pump system from 6 to 10 °C, the exergy efficiency increases from 38.2% to 39.4% and the exergy destruction rate decreases from 2550 kW to 2375 kW. As expected, a rise in glycol–water temperature means higher heat energy absorbed from the ground and transferred to the system. The inlet glycol–water temperature is possibly the single most acting variable of the BTES system.

The variation of the overall exergy destruction of the system by varying the evaporator and condenser temperature is presented in Figs. 8 and 9. It can be seen from these figures that the patterns are almost identical but in a reverse form. Exergy destruction rate decreases when the evaporator temperature increases. This is because of a temperature difference decrease between condenser and evaporator. Thus, higher evaporator temperatures have more energy which is transferred to the process. Also, exergetic efficiency of the overall system increases with evaporator temperature. The variation of these parameters with condenser temperature is vice versa.

Fig. 10 shows the variation of exergy destruction and exergetic efficiency with excess air ratio. It is clear from the figure that with the increase of excess air ratio, exergy destruction rate increases and exergetic efficiency decreases. Therefore, it should be provided a complete and proper combustion in the boilers since an increase in air ratio causes higher exergy destruction rates. As declared previously in third part of this study, the combustion in the boilers is assumed to be complete for the general analysis, but for a comparative study, it is changed between 10% and 20% for examining the trends of exergy destruction.

In Fig. 11, the variation of exergy destruction and exergetic efficiency with product temperature of the boilers is presented. From the figure, the increase of product temperature increase exergy destruction rate and exergetic efficiency. The higher product temperature causes higher heat energy losses to the environment. Thus, higher heat energy loses through flue gases increase the exergy destruction in the boilers. Therefore, decreasing the temperature of the flue gases (i.e. heat recovery) can help to improve the exergetic efficiency of the boilers.

Fig. 12 shows the graphical representation of the exergy balance (so-called Grassmann diagram) for the GSHP system supported with boilers. The Grassmann diagram gives quantitative information regarding the proportion of the exergy input to the plant, which is dissipated in the different system components [20]. The proportion of the exergy inputs to the system those are dissipated in each of the components are clearly seen from the figure.

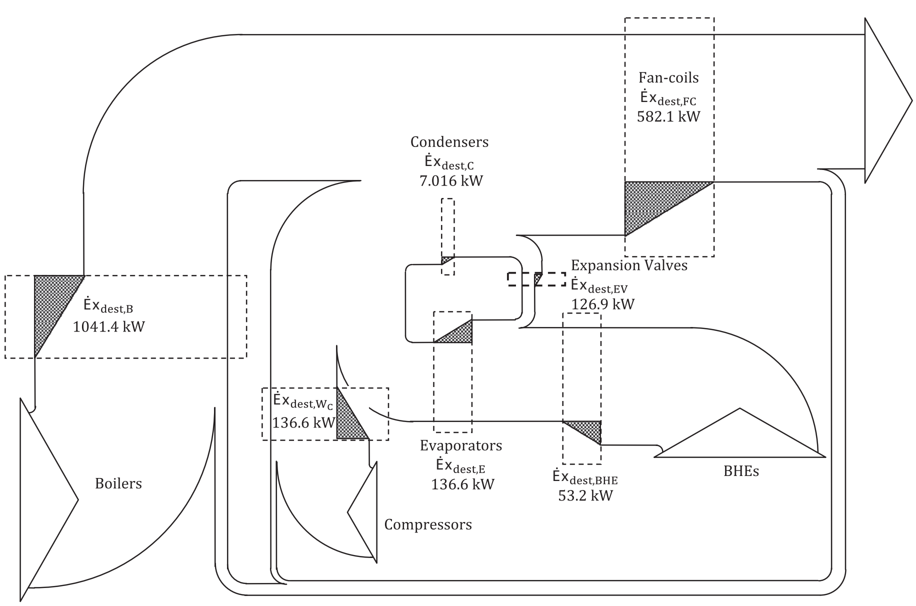

Fig. 12. Exergy balance diagram (Grassmann diagram) for the heating system.

5. Conclusions

The borehole thermal energy storage system linked with HVAC system of University of Ontario Institute of Technology is thermodynamically analyzed for heating applications of campus buildings. Some actual data of heating loads are used to evaluate system performance using thermodynamic concepts. As performance indicators, values of COP_{HP}, boiler efficiency and exergy efficiency of the system are analyzed for different operating conditions. Parametric studies are also carried out for comparison purposes. The results show that for the heating system, exergy efficiency increases slightly when the inlet temperature of glycol–water mixture increases. Also, with the increase of reference environment temperature results in decrease of exergy efficiency for the heating system. Furthermore, the overall system's exergy destruction rate and exergy efficiency are determined as 2384.2 kW and 41.35% respectively. In brief, considerable energy savings can be achieved by determining and reducing the exergy destructions of all system components. Also, we plan to perform a thermoeconomic analysis, which involves exergy and economic parameters as a future study.

Acknowledgments

The authors would like to thank Scientific and Technological Research Council of Turkey (TUBITAK) for the financial support provided to Dr. Onder Kizilkan for his visit to UOIT, and the University of Ontario Institute of Technology (UOIT) for the technical assistance.

References

[1] ECBCS Annex 49. Low exergy systems for high-performance buildings and communities. midterm report. <http://www.annex49.info/download/midterm_report.pdf> [accessed 03.03.20].
[2] Dincer I, Rosen MA. Thermal energy storage systems and applications. 2nd ed. United Kingdom: John Wiley & Sons; 2011.
[3] Caliskan H, Dincer I, Hepbasli A. Thermoeconomic analysis of a building energy system integrated with energy storage options. Energy Convers Manage 2013;76:274–81.
[4] Dincer I. Thermal energy storage as a key technology in energy conservation. Int J Energy Res 2002;26(7):567–88.
[5] Yeung KWD. Enhancements to a ground loop heat exchanger design program. Master Thesis, Graduate College of the Oklahoma State University; 1996.
[6] Esen H, Inalli M, Esen M, Pihtili K. Energy and exergy analysis of a ground-coupled heat pump system with two horizontal ground heat exchangers. Build Environ 2007;42:3606–15.
[7] Jun L, Xu X, Jun G, Jie Y. Evaluation of heat exchange rate of GHE in geothermal heat pump systems. Renewable Energy 2009;34:2898–904.
[8] Marzbanrad J, Sharifzadegan A, Kahrobaeian A. Thermodynamic optimization of GSHPS heat exchangers. Int J Thermodyn 2007;10:107–12.
[9] Gustafsson AA, Westerlund L, Hellström G. CFD-modelling of natural convection in a groundwater-filled borehole heat exchanger. Appl Therm Eng 2010;30:683–91.
[10] Ozgener L, Hepbasli A, Dincer I. Energy and exergy analysis of Salihli geothermal district heating system in Manisa, Turkey. Int J Energy Res 2005;29:393–408.
[11] Sakulpipatsin P, Itard LCM, Van der Kooi HJ, Boelman EC, Luscuere PG. An exergy application for analysis of buildings and HVAC systems. Energy Build 2010;42:90–9.
[12] Zhai XQ, Yang Y. Experience on the application of a ground source heat pump system in an archives building. Energy Build 2011;43:3263–70.
[13] Urchueguía JF, Zacarés M, Corberán JM, Montero MartosJÁ, Wittec H. Comparison between the energy performance of a ground coupled water to water heat pump system and an air to water heat pump system for heating and cooling in typical conditions of the European Mediterranean coast. Energy Convers Manage 2008;49:2917–23.
[14] Sharqawy MH, Mokheimer EM, Habib MA, Badr HM, Said SA, Al-Shayea NA. Energy, exergy and uncertainty analyses of the thermal response test for a ground heat exchanger. Int J Energy Res 2009;33:582–92.
[15] Wu W, You T, Wang B, Shi W, Li X. Evaluation of ground source absorption heat pumps combined with borehole free cooling. Energy Convers Manage 2014;79:334–43.
[16] UOIT Project records for GSPH system; 2004.
[17] Keen Engineering. UOIT/Durham College GSHP Project Report. March; 2003.
[18] Beatty B, Thompson J. 75 Km of Drilling for thermal energy storage. Technical report for BTES system installed in UOIT/Durham College; 2004.
[19] Dincer I, Rosen MA. A unique borehole thermal storage system at university of Ontario institute of technology. In: Paksoy HO (Ed.), Thermal energy storage for sustainable energy consumption, NATO Science Series; 2007. p. 221–8.
[20] Kotas TJ. The exergy method of thermal plant analysis. Florida: Krieger; 1985.
[21] Saidur R, Ahamed JU, Masjuki HH. Energy, exergy and economic analysis of industrial boilers. Energy Policy 2010;38:2188–97.
[22] Rosen MA, Dincer I. Effect of varying dead-state properties on energy and exergy analyses of thermal systems. Int J Therm Sci 2004;43:121–33.

View publication stats